Supplemental Materials

Supplementary Methods:

Cell culture, miR mimics/ siRNA transfection, lentiviral over-expression and treatments Human dermal microvascular endothelial cells (HDMECs) were cultured under standard conditions (37°C in a humidified atmosphere consisting of 95% air and 5% CO2) in MCDB-131 medium supplemented with 10% FBS, 10 mM L-glutamine and 100 IU/mL penicillin, 0.1 mg/mL streptomycin, (Invitrogen) as described previously.[1] Primary adult human dermal microvascular endothelial cells (HDMECs) were grown at 37°C, 95% air and 5% CO2 in EBM-2 medium (Lonza) supplemented with EGM-2MV single quotes (Lonza) as described previously.[1] HEK-293 cells were cultured in humidified chamber (37°C, 95% air and 5% CO2) with DMEM medium supplemented with 10% FBS and 100 IU/mL penicillin, 0.1 mg/mL streptomycin. One day before transfection, cells were seeded in 12-well plate at density 0.15 x 10^6 cells/well. Confluence will reach approximately 70% at the time of transfection. Transfection was achieved by liposome-mediated delivery of miR-200b mimic (20nM), miR-200b inhibitor (100 nM) or siRNA smart pool for human GATA2, VEGFR2 and p53 (100nM) using DharmaFECTTM 1 transfection reagent (Dharmacon RNA Technologies) and OptiMEM serum-free medium (Invitrogen). All the miR mimics, inhibitors and siRNA were obtained from Dharmacon RNA Technologies. Supplementary table I shows the corresponding sequences of siRNA employed in this study. Cells were either harvested directly or seeded on Matrigel® pre-coated plates for further analysis after 72-h transfection unless specified. For lentiviral over-expression studies, HDMECs were infected with lentiviral particles carrying miR-200b resistant form of GATA2 or VEGFR2 at different MOI (from 0.1 to 1) for 48 hours. Medium were refreshed and cells were allow to grow for another 48 hours. Protein was extracted for Western blot to validate the transduction efficiency. Both GATA2 and VEGFR2 over-expression lentivirus were obtained from Applied Biological Materials. For Matrigel® study, medium was removed after 48h transduction

and cells were then transfected with miR-200b mimic (20nM) for another 48 hours. Cells were seeded on Matrigel® pre-coated plates to study the tube formation ability. For TNF-α treatment, HDMECs or primary HDMECs were seeded in 12-well plate at density 0.15 x 10^6 cells/well. Medium were refreshed and recombinant human TNF-α (R & D system) at 50 ng/ml or vehicle (1% BSA in PBS) were added to the cells according to the previous study.[2] Cells were collected for RNA or protein at the time indicated. For the TNF-α -miR-200b inhibitor study, cells were first transfected with control or anti-miR-200b (100nM) for 48 hours, followed by treatment with either vehicle or TNF-α. After 24 hours, cells were either lyzed for protein/ RNA extraction or plated on Matrigel® pre-coated plate for further analysis.

Luciferase reporter construct The reporter constructs pLu-GATA2-3'UTR, pLu-VEGFR2-3'UTR and their mutant form were obtained from Signosis. The constructs were designed based on the sequence of miR-200b binding site and a total of 251bp (for both pLu- wild type GATA2-3'UTR and pLu- mutated GATA2-3'UTR), 496bp (pLu- wild type VEGFR2-3'UTR) or 432 bp (pLu- mutated VEGFR2-3'UTR) were cloned in the 3'UTR of pLuc plasmid. Firefly luciferase was cloned under the control of CMV promoter. For mutated construct, the seed sequence regions were replaced to non-sense sequence (for details, please see Supplementary Figure V).

miR target reporter luciferase assay HEK-293 cells were transfected with 100ng pLuc-GATA2-3'UTR, pLuc-VEGFR2-3'UTR plasmid or their corresponding mutant construct (Supplementary Figure V) using lipofectamine TM LTX/ plus reagent (Invitrogen) according to the manufactures protocol.[1] Normalization was achieved by co-transfection with renilla plasmid (10ng). Cells were lyzed after 48 hours and luciferase activity was determined using dual-luciferase reporter assay system (Promega). Data are presented as ratio of firefly to renilla luciferase activity (FL/RL).

RNA extraction and quantitative real-time PCR RNA from cells or murine wound sample was extracted using miRVana miRNA Isolation Kit according to the manufactures protocol (Ambion). RNA was first reverse-transcribed using Taqman MicroRNA Reverse Transcription Kit (Applied Biosystems), followed by semi-quantitative real time PCR using Universal PCR Master Mix and specific Taqman miR primers (Applied Biosystems) as described previously.[1,3]

Western blots Western blot was performed using antibodies against GATA2 (Santa Cruz biotechnology) and VEGFR2 (Cell Signaling) as described previously.[1] Briefly, the cells were lyzed in lysis buffer containing 10mM Tris pH 7.4, 150mM NaCl, 1% Triton X-100, 1% deoxycholic acid, 0.1 % SDS and 5mM EDTA. Cell lysates were resolved in SDS-PAGE, transblotted to PVDF membrane (Amersham), blocked in 10% skim milk and incubated with primary antibody against either GATA2 (1: 5,000) or VEGFR2 (1: 2,000) overnight at 4^{o}C. Signal was visualized using corresponding HRP-conjugated secondary antibody (Amersham, 1:3,000) and ECL Plus™ Western Blotting Detection Reagents (Amersham). β-actin (Sigma, 1: 7, 000) serves as loading control.

Immunohistochemistry (IHC) and immunocytochemistry (ICC) Immunostaining of GATA2, VEGFR2 and CD31 was performed on cryosections of wound sample using specific antibodies as described previously.[4] Briefly, OCT embedded tissue were cryosectioned at 10μm thick, fixed with cold acetone, blocked with 10% normal goat serum and incubated with specific antibodies against CD31 (BD Bioscience, 1:400) and GATA2 (Santa Cruz biotechnology, 1:2,000) or VEGFR2 (Santa Cruz biotechnology, 1:200) overnight at 4°C. Signal was visualized by subsequent incubation with fluorescence-tagged secondary antibodies (FITC-tagged α-rat, 1:200; Alexa 568-tagged α-rabbit, 1:200). Images were captured by microscope and quantification of fluorescent intensity of image was achieved by software AxioVision Rel 4.6 (Carl Zeiss Microimaging). For ICC, cells were fixed with

paraformaldehyde, permeabilized with 0.1% TritonX-100, blocked with 10% normal goat serum and incubated with primary antibody against GATA2 (1:3,000) and VEGFR2 (1:200) overnight as described previously.[1] Signal was visualized using Alexa Fluor® 488 dye-conjugated antibody against rabbit (Invitrogen, 1:200), counterstained with DAPI. Images were captured by microscope using software AxioVision Rel 4.6 (Zeiss).

Matrigel® tube formation assay *In vitro* angiogenesis was determined by tube formation ability on Matrigel® as described previously.[1] Cells were plated out after transfection or treatment and seeded on Matrigel® pre-coated 4-well plate at density 5 x 10^4 cells/ well. The angiogenic property was assessed 8 hours after seeding, and the tube length was measured using the software AxioVision Rel 4.6 (Zeiss).

LCM Laser capture microdissection was performed using the laser microdissection system from PALM Technologies (Bernreid, Germany) containing a PALM MicroBeam and RoboStage for high-throughput sample collection and a PALM RoboMover (PALM Robo software, Version 2.2) as described previously.[5] For immunofluorescence-directed LCM, blood vessels were stained with CD31 antibody (1:25), FITC-conjugated secondary antibody (1:200), and subsequently visualized using fluorescent lamp. For dermal LCM, sections were stained with hematoxylin for 30s, subsequently washed with DEPC-H_2O and dehydrated in ethanol. Dermal fraction was identified based on the histology. Blood vessel or dermal fraction were typically cut and captured under a 20× ocular lens, using Cut elements. The samples were catapulted into 25 µl of cell direct lysis extraction buffer (Invitrogen). Approximately 250,000 μm^2 of tissue area was captured into each cap and the extract was then held at −80°C for extraction process.

Laser Doppler Dermal blood flow was analyzed by laser Doppler imaging device as described previously.[4] Briefly, mice with d7 skin wounds were anesthetized with isoflurane. The MoorLDI-Mark 2 laser Doppler blood perfusion imager (resolution: 256 × 256 pixels, visible red laser beam at 633 nm) was used for mapping tissue blood flow as reported previously. [4]

Statistical Analyses

Data reported represent means $\pm$ SEM. Difference between two means was tested by Student t-test while one-way ANOVA analysis was employed to compare three groups or more. $P<0.05$ was considered as statistical significance.

Supplementary References:

1. Chan YC, Khanna S, Roy S, Sen CK. Mir-200b targets ets-1 and is down-regulated by hypoxia to induce angiogenic response of endothelial cells. *J Biol Chem*. 2011;286:2047-2056
2. Chen JX, Chen Y, DeBusk L, Lin W, Lin PC. Dual functional roles of tie-2/angiopoietin in tnf-alpha-mediated angiogenesis. *Am J Physiol Heart Circ Physiol*. 2004;287:H187-195
3. Pospisil V, Vargova K, Kokavec J, Rybarova J, Savvulidi F, Jonasova A, Necas E, Zavadil J, Laslo P, Stopka T. Epigenetic silencing of the oncogenic mir-17-92 cluster during pu.1-directed macrophage differentiation. *EMBO J*. 2011
4. Biswas S, Roy S, Banerjee J, Hussain SR, Khanna S, Meenakshisundaram G, Kuppusamy P, Friedman A, Sen CK. Hypoxia inducible microrna 210 attenuates keratinocyte proliferation and impairs closure in a murine model of ischemic wounds. *Proc Natl Acad Sci U S A*. 2010;107:6976-6981
5. Roy S, Patel D, Khanna S, Gordillo GM, Biswas S, Friedman A, Sen CK. Transcriptome-wide analysis of blood vessels laser captured from human skin and chronic wound-edge tissue. *Proc Natl Acad Sci U S A*. 2007;104:14472-14477

Supplementary Table I:

Sequence of siRNAs employed in this study:

siRNA	
GATA2 siRNA	5'-GCAAGGCUCGUUCCUGUUC-3' 5'-GAAGGGAUCCAGACUCGGA-3' 5'-GCACAAUGUUAACAGGCCA-3' 5'-GGGCAGAACCGACCACUCA-3'
VEGFR2 siRNA	5'-GCGAUGGCCUCUUCUGUAA-3' 5'-GGAAAUCUCUUGCAAGCUA-3' 5'-CUACAUUGUUCUUCCGAUA-3' 5'-GGGCAUGUACUGACGAUUA-3'
p53 siRNA	5'-GAAAUUUGCGUGUGGAGUA-3' 5'-GUGCAGCUGUGGGUUGAUU-3' 5'-GCAGUCAGAUCCUAGCGUC-3' 5'-GGAGAAUAUUUCACCCUUC-3'

Supplemental Figure Legends

Supplementary Figure I. Down-regulation of endothelial miR-200a was evidenced during cutaneous wound healing. Quantitative PCR analysis of miR-200a expression of **(A)** day 3 and day 7 wound edge tissue (8x 16mm full-thickness excisional wounds, n=5) and **(B)** laser microdissected endothelial cells (n=3) from d3 wounds, compared to their respective control skin sample. Results are mean $\pm$ SEM. * indicates $p<0.05$ compared to respective control.

Supplementary Figure II. Wound-induced repression of miR-200b was not evident in epidermis or non-endothelial dermal tissue element in cutaneous wound healing. Quantitative PCR analysis of miR-200b expression of laser microdissected **(A)** epidermal or **(B)** non-endothelial dermal tissue element from d3 wound-edge tissue compared to their respective control skin sample. Results are mean $\pm$ SEM. N.S= not statistically significant

Supplementary Figure III. Intradermal delivery of miR-200b over-expressing lentivirus induced miR-200b expression in the dermis of murine skin. **(A)** Representative diagram shows LCM of dermal fraction before collection and after collection. **(B)** Quantitative PCR analysis of miR-200b expression of laser microdissected dermal fraction 3 days after delivery of control or miR-200b over-expressing lentivirus (2×10^7 cfu/ml, 50µl per site) (n=6). Results are mean $\pm$ SEM. * indicates $p<0.05$ compared to control lentivirus. .

Supplementary Figure IV. Wound closure response following treatment with miR-200b or control miR over-expressing lentiviral vector. Wounds were treated with miR-200b over-expressing lentiviral or control particles as described in Materials. Wound closure was monitored by digital planimetry and was presented as % of wound closure (n=4). Results are mean ± SEM. *** indicates $p<0.001$, * indicates $p<0.05$ compared to respective control.

Supplementary Figure V. Predicted binding sites of miR-200b and the sequence of reporter construct. Bioinformative analysis of possible binding sites of **(A)** GATA2 and **(B)** VEGFR2 3'UTR for miR-200b using algorithms including Targetscan, Pictar, miRDB, miRanda and Diana-microT (upper panel). Sequence of wild type GATA2 3'UTR (middle panel, **A**) and GATA2 3'UTR with the mutation of predicted binding site (lower panel, **A**) cloned in the reporter construct. Sequence of wild type VEGFR2 3'UTR (middle panel, **B**) and the corresponding 3'UTR with the mutation of predicted binding sites (lower panel, B) cloned in the reporter construct. The predicted binding sites are the underlined sequences with mutated sequence shown in *italic*. All reporter construct were cloned by Signosis.

Supplementary Figure VI. miR-200b negatively regulated GATA2 and VEGFR2 expression in primary HDMECs Western blot analysis of **(A)** GATA2 and **(B)** VEGFR2 protein expression in miR-200b mimic delivered primary HDMECs (n=3). β-actin serves as loading control. Results are mean ± SEM. *** indicates $p<0.001$ compared to control mimic.

Supplementary Figure VII. miR-200b mimic delivery induced loss of both GATA2 and VEGFR2, and inhibits angiogenesis *in vitro*. **(A)** Representative diagram shows GATA2 (left) or VEGFR2 (right) immunocytochemistry, counterstained with DAPI, after miR-200b mimic delivery in HDMECs from

three independent experiments. **(B)** Representative diagram shows Matrigel® tube formation at 8 h in HDMEC treated with control mimic or miR-200b mimic from three independent experiments.

Supplementary Figure VIII. GATA2 and VEGFR2 knockdown exerted angiostatic effects on HDMECs. Western blot analysis of **(A)** GATA2 and **(B)** VEGFR2 protein expression in corresponding siRNAs delivered HDMECs (n=3). β-actin serves as loading control. Results are mean ± SEM. *** indicates $p<0.001$, ** indicates $p<0.01$ compared to control siRNA . Matrigel® tube formation at 8 h in **(C)** GATA2 or **(D)** VEGFR2 siRNA-transfected HDMECs (n=3). Results are mean ± SEM. *** indicates $p<0.001$, ** indicates $p<0.01$ compared to respective control.

Supplementary Figure IX Over-expression of GATA2 or VEGFR2 induced GATA2 or VEGFR2 expression, respectively Western blot analysis of **(A)** GATA2 and **(B)** VEGFR2 protein expression after lentiviral over-expression of GATA2 and VEGFR2, respectively in HDMECs (n=3). β-actin serves as loading control. ** indicates $p<0.01$, * indicates $p<0.05$ compared to respective control.

Supplementary Figure X. Simultaneous over-expression of GATA2 and VEGFR2 induced angiogenic response additively. Matrigel® tube formation at 8 h in HDMEC treated with control mimic, miR-200b mimic and miR-200b with GFP control over-expression, GATA2 over-expression, VEGFR2 over-expression or simultaneous over-expression of both GATA2 and VEGFR2 (n=3). Results are mean ± SEM. *** indicates $p<0.001$ compared to respective control miR, $^{+}$ indicates $p<0.05$ while $^{+++}$ represent $p<0.001$ compared to GFP control. ### indicate $p<0.001$ compared to GATA2 over-expression alone. N.S= not statistically significant.

Supplementary Figure XI. VEGFR2 served as a mediator of GATA2-associated angiogenesis. **(A)** Western blot analysis of VEGFR2 protein expression in GATA2 knockdown HDMECs. β-actin serves a loading control (n=3). **(B)** Western blot analysis of VEGFR2 protein expression in miR-200b mimic delivery with or without GATA2 over-expresssion. β-actin serves a loading control (n=3). (**C)** Representative diagram and quantification of tube formation (% of control) showing Matrigel® tube formation at 8 h in HDMEC treated with control siRNA, GATA2 siRNA and GATA2 siRNA + lentivirial VEGFR2 over-expression (n=4). Results are mean ± SEM. *** indicates p<0.001, ** indicates p<0.01, * indicates p<0.05 compared to respective control treated cells. $^{++}$ represent p<0.01 compared to GATA2 siRNA alone.

Supplementary Figure XII. Diabetic mice exhibited impaired wound angiogenesis. Wound angiogenesis, as depicted by **(A)** cutaneous blood flow measured by laser Doppler (n=5) and **(B)** microvessle counts measured by CD31-immunostaining (n=5) at day 7 post-wounding. Results are mean ± SEM. *** indicates p<0.001, ** represents p<0.01 compared to m+/db non-diabetic wounds.

Supplementary Figure XIII. TNF-α treatment induced miR-200b expression and suppresses protein expression of GATA2 and VEGFR2 in primary HDMECs. (A) Quantitative PCR analysis of miR-200b expression after treatment of TNF-α for 24h in primary HDMECs. **(B)** Western blot analysis of GATA2 and VEGFR2 protein expression in TNF-α-treated primary HDMECs. β-actin serves as loading control (n=4). Results are mean ± SEM. *** indicates p<0.001, ** indicates p<0.01 compared to vehicle treated cells.

Supplementary Figure XIV. Delivery of anti-miR-200b reversed TNF-α-dependent miR-200b induction HDMECs. Quantitative PCR analysis of miR-200b expression after treatment of TNF-α for 24h in presence of absence of anti-miR-200b (n=4). Results are mean ± SEM. * indicates $p<0.05$ compared to vehicle treated cell, $^{++}$ indicates $p<0.01$ compared to TNF-α + control anti-miR.

Supplementary Figure XV. Neutralization of TNF-α improved wound closure in diabetic mice. Wounds were induced in m+/db non-diabetic mice, db/db diabetic mice treated with placebo, and db/db diabetic mice treated with sTNFR1 as described in *Methods*. Wound closure was monitored on day 1, 3, 5, 7, 9, and 11 post-wounding and was presented as % of wound closure (n=6). Results are mean ± SEM. *** indicates $p<0.001$, ** indicates $p<0.01$ compared to m+/db non-diabetic mice, $^{+++}$ indicates $p<0.001$, $^{++}$ indicates $p<0.01$ and $^{+}$ indicates $p<0.05$ compared to db/db diabetic mice treated with placebo

Supplementary Figure XVI. Knockdown of p53 attenuated TNF-α induced induction of miR-200a, miR-200b and miR-429 in HDMECs. Quantitative PCR analysis of **(A)** miR-200a, **(B)** miR-200b, and **(C)** miR-429 expression after treatment of TNF-α for 24h in HDMECs in the presence or absence of p53 siRNA. Results are mean ± SEM. ** indicates $p<0.01$ compared to vehicle-treated cells, $^{+}$ indicates $p<0.05$ compared to TNF-α alone.

Supplementary Figure XVII. Summary depicting the identified miR-200b-dependent molecular mechanisms implicated in wound angiogenesis. In diabetic wounds excessive TNF-α induced miR-200b expression leading to silencing of angiogenic GATA2 and VEGFR2, resulting in impairment in wound healing. VEGFR2 was further down-regulated by a direct repression of GATA2.

Supplemental Figure I

(A)

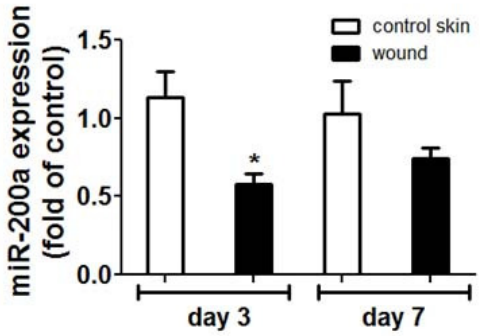

(B)

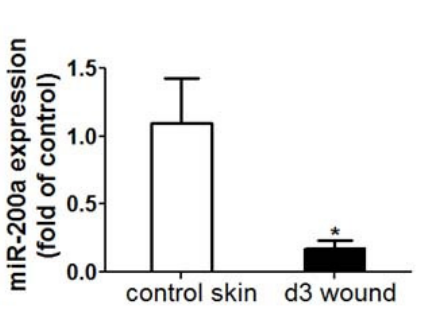

Supplemental Figure II

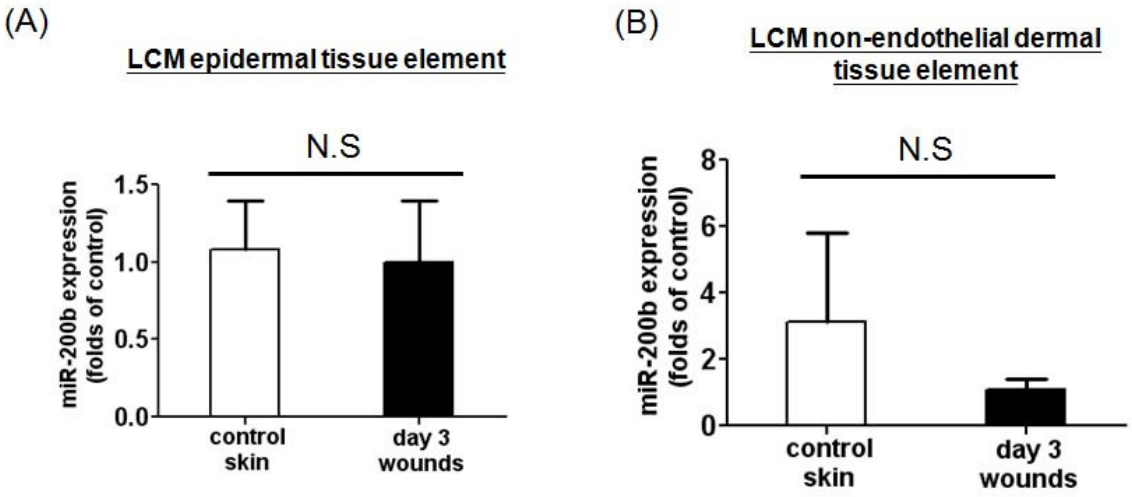

Supplemental Figure III

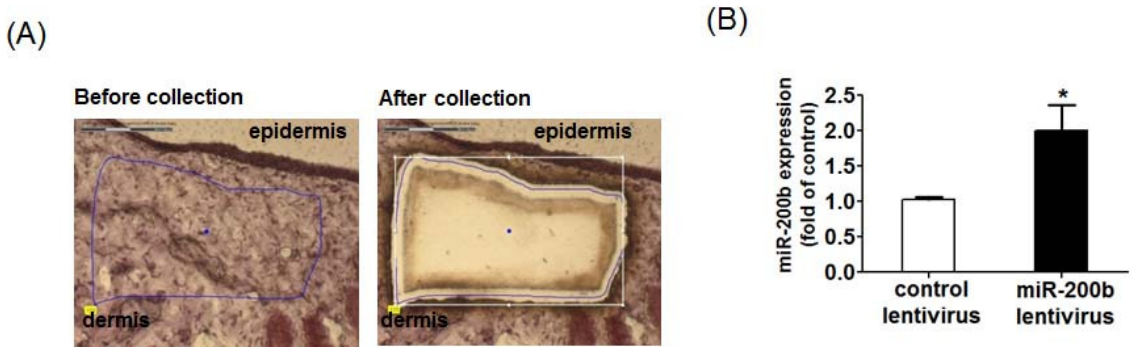

Supplemental Figure IV

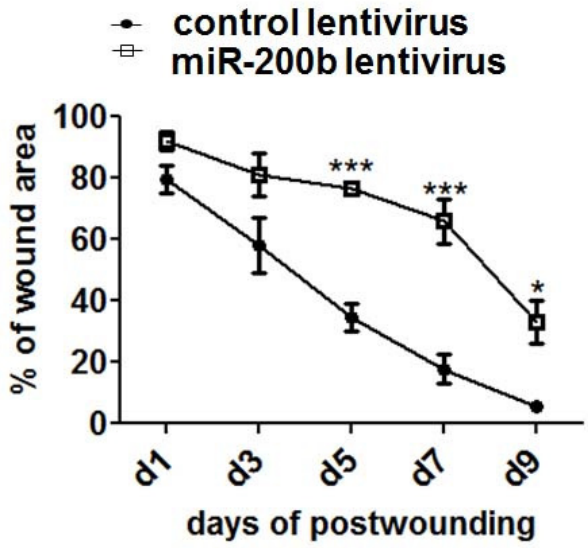

Supplemental Figure V

(A)

Position 1424-1430 of GATA2 3' UTR

5' ...AAGAAAAAGAAUCGGCAGUAUUU...
hsa-miR-200b 3' AGUAGUAAUGGUCCGUCAUAAU

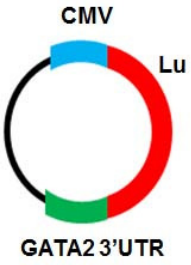

Wild type GATA2 3'UTR

5' -
GCAGTCGCTGCAGGGAGCACCACGGCCAG
AAGTAACTTATTTTGTACTAGTGTCCGCATAA
GAAAAAGA**ATCGGCAGTATT**TTCTGTTTTTA
TGTTTTATTTGGCTTGTTTTATTTTGGATTAGT
GAACTAAGTTATTGTTAATTATGTA- 3'

Mutated GATA2 3'UTR

5' -
GCAGTCGCTGCAGGGAGCACCACGGCCAG
AAGTAACTTATTTTGTACTAGTGTCCGCATAA
GAAAAAGA*TAGCCGTCATAA*TTCTGTTTTTAT
GTTTTATTTGGCTTGTTTTATTTTGGATTAGT
GAACTAAGTTATTGTTAATTATGTA- 3'

(B)

Position 1028-1034 of VEGFR2 3' UTR

5' ... CACCCCGCAACCCAUCAGUAUUU...
hsa-miR-200b 3' AGUAGUAAUGGUCCGUCAUAAU

Position 1380-1386 of VEGFR2 3' UTR

5' ...AUUCACAUUUUGUAUCAGUAUUA...
hsa-miR-200b 3' AGUAGUAAUGGUCCGUCAUAAU

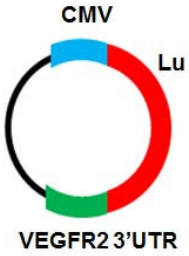

Wild type VEGFR2 3'UTR

5' –
GTTCAATGTGAAGCTGTGTGTGGTGTCAAAGTTTCAGGAAGGATTTTACCCTTTT
GTTCTTCCCCCTGTCCCCAACCCACTCTCACCCCGCAACCCAT**CAGTATT**TTAG
TTATTTGGCCTCTACTCCAGTAAACCTGATTGGGTTTGTTCACTCTCTGAATGATT
ATTAGCCAGACTTCAAAATTATTTTATAGCCCAAATTATAACATCTATTGTATTATTTA
GACTTTTAACATATAGAGCTATTTCTACTGATTTTTGCCCTTGTTCTGTCCTTTTTT
TCAAAAAAGAAAATGTGTTTTTTGTTTGGTACCATAGTGTGAAATGCTGGGAACA
ATGACTATAAGACATGCTATGGCACATATATTTATAGTCTGTTTATGTAGAAACAAA
TGTAATATATTAAAGCCTTATATATAATGAACTTTGTACTATTCACATTTTGTAT**CAGT**
ATTATGTAGCATAACAAAGGTCATAATGCTTTCAGCAATTGATG-3'

Mutated VEGFR2 3'UTR

5'
CCTGTCCCCAACCCACTCTCACCCCGCAACCCAT*GTCATAA*TTAGTTATTTGGCC
TCTACTCCAGTAAACCTGATTGGGTTTGTTCACTCTCTGAATGATTATTAGCCAGA
CTTCAAAATTATTTTATAGCCCAAATTATAACATCTATTGTATTATTTAGACTTTTAAC
ATATAGAGCTATTTCTACTGATTTTTGCCCTTGTTCTGTCCTTTTTTTCAAAAAAGA
AAATGTGTTTTTTGTTTGGTACCATAGTGTGAAATGCTGGGAACAATGACTATAAG
ACATGCTATGGCACATATATTTATAGTCTGTTTATGTAGAAACAAATGTAATATATTA
AAGCCTTATATATAATGAACTTTGTACTATTCACATTTTGTAT*GTCATAA*ATGTAGCA
TAACAAAGGTCATAATGCTTTCAGCAATTGATG-3'

Supplemental Figure VI

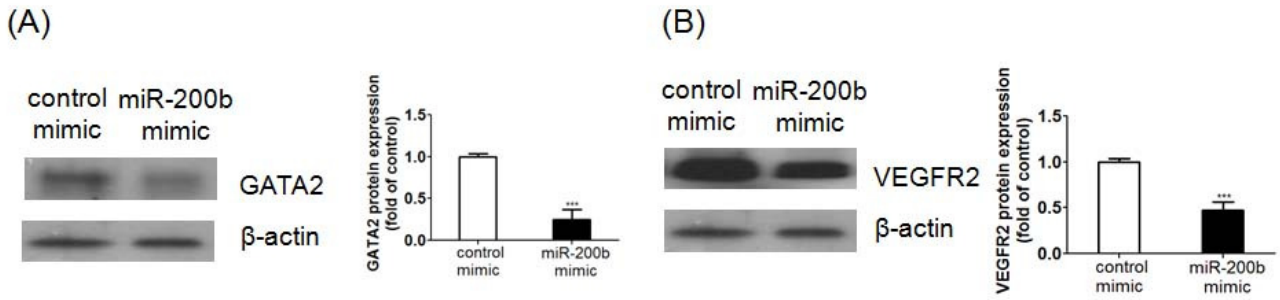

Supplemental Figure VII

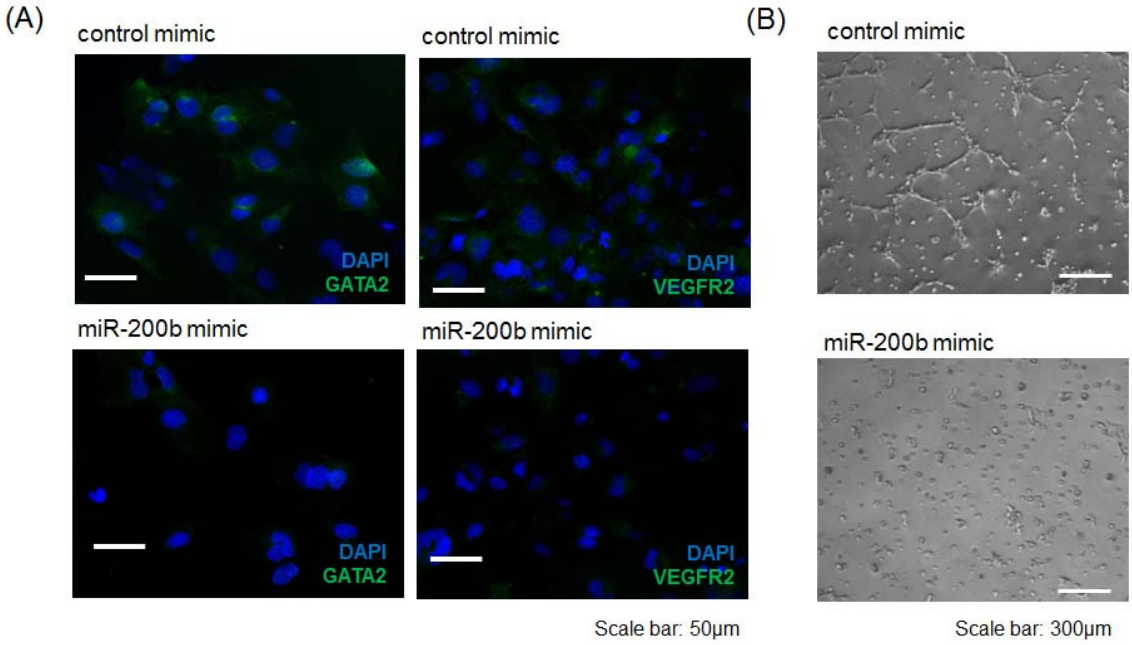

Supplemental Figure VIII

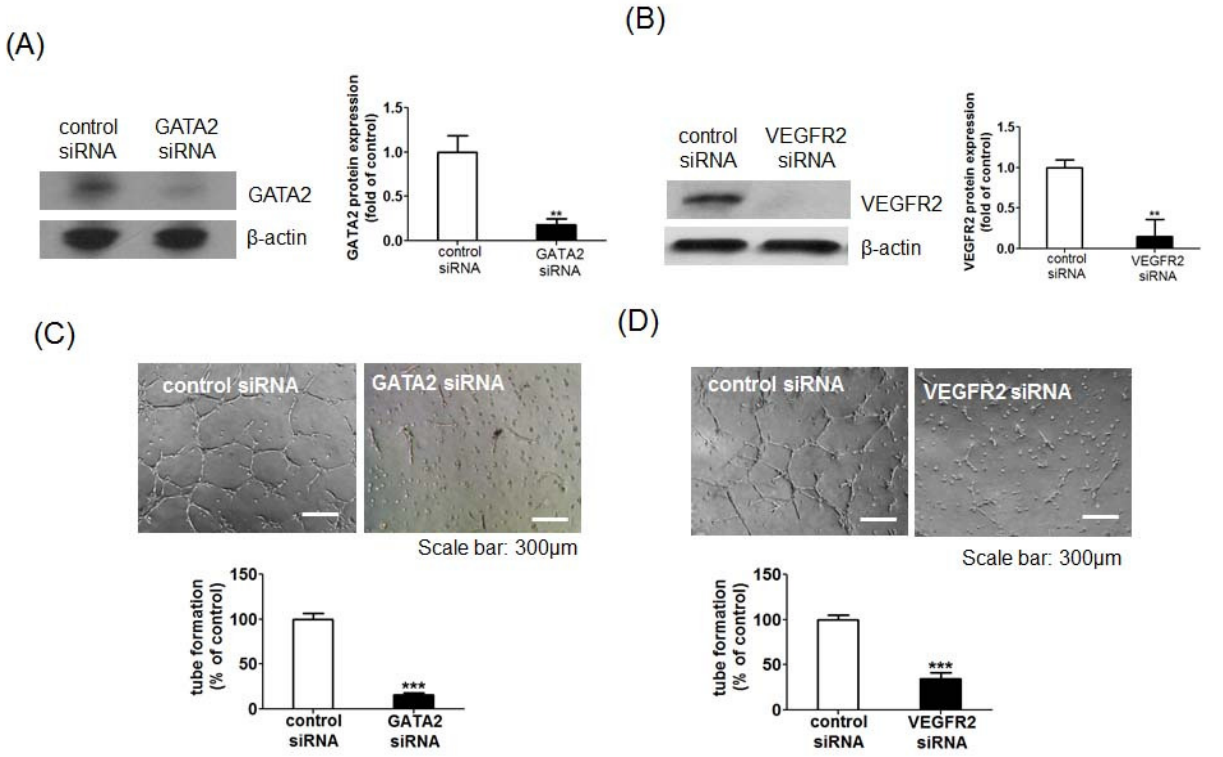

Supplemental Figure IX

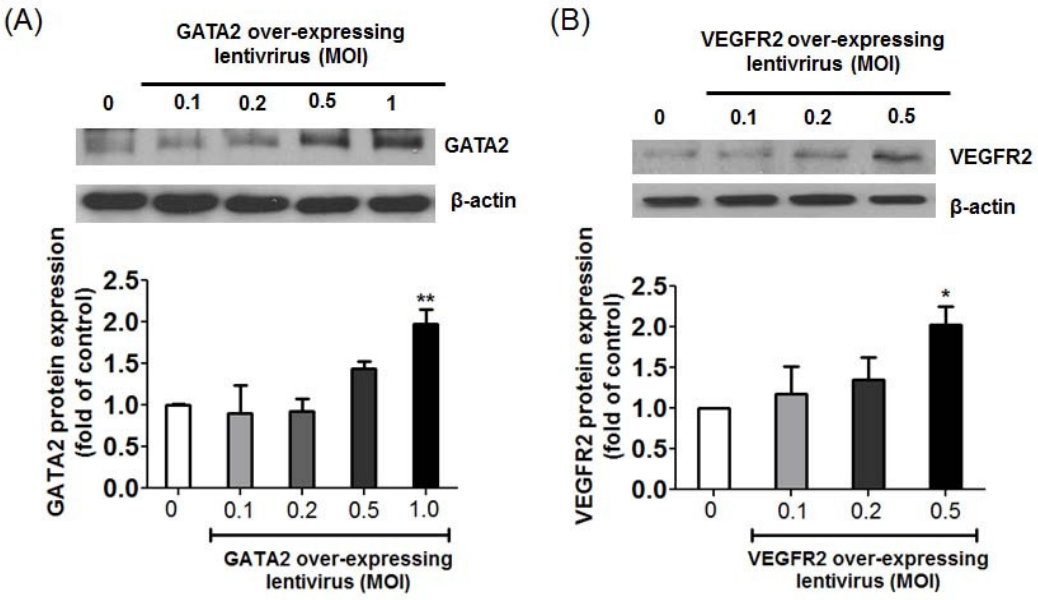

Supplemental Figure X

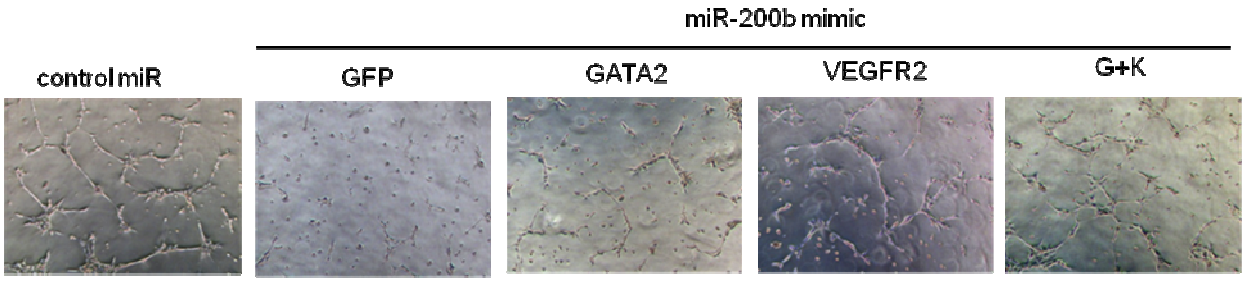

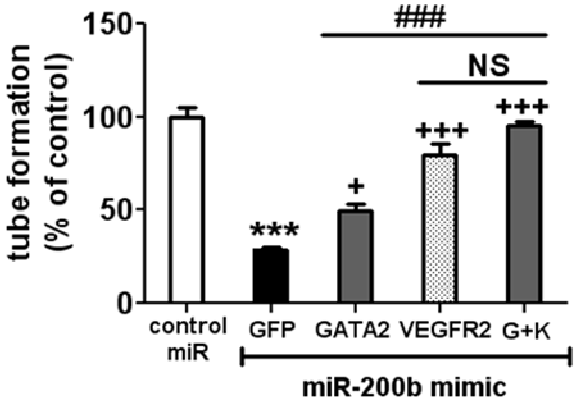

GFP- control GFP lentivirus
GATA2- GATA2 over-expressing lentivirus
VEGFR2- VEGFR2 over-expressing lentivirus
G+K- GATA2 over-expressing lentivirus + VEGFR2 over-expressing lentivirus

Supplemental Figure XI

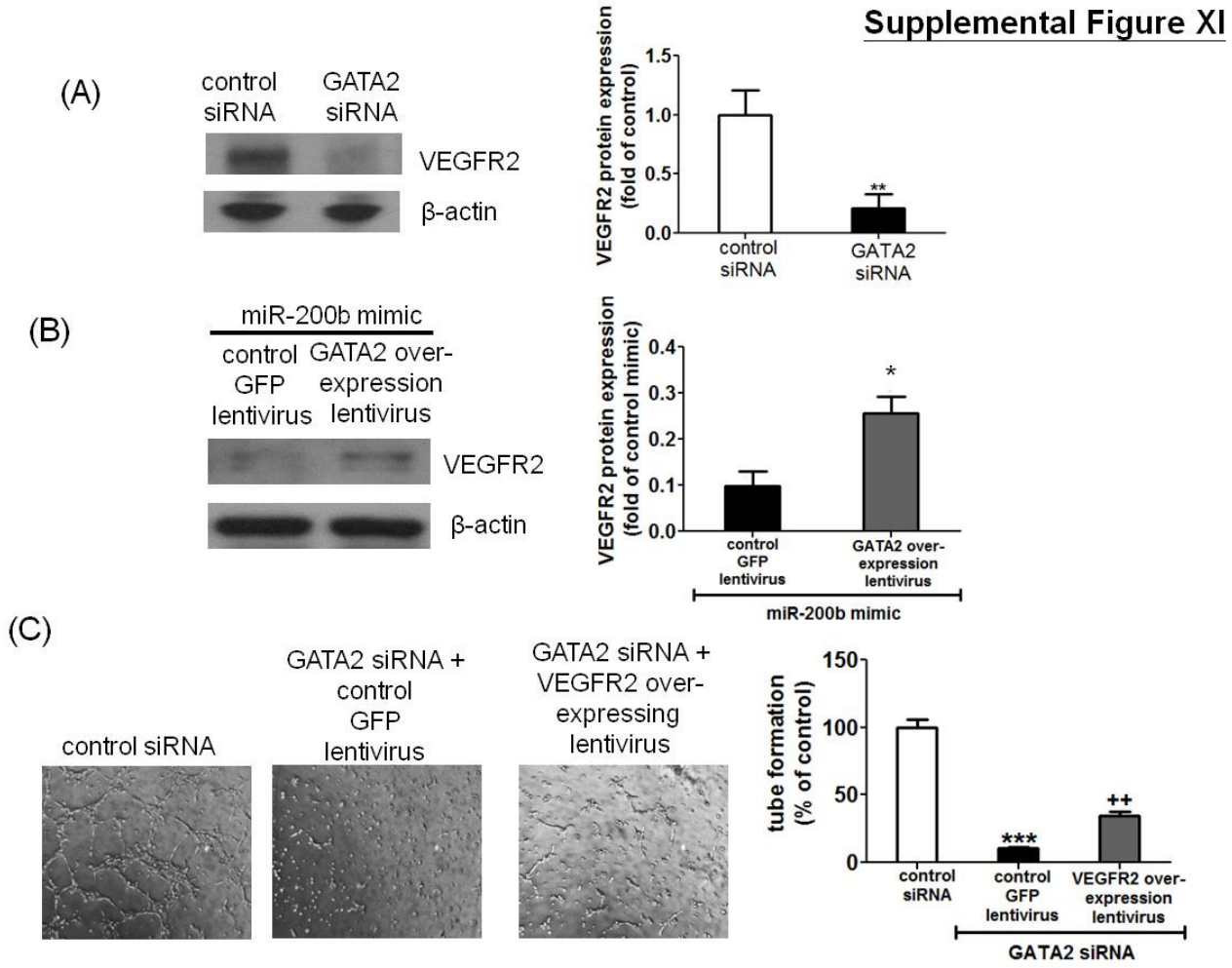

Supplemental Figure XII

(A)

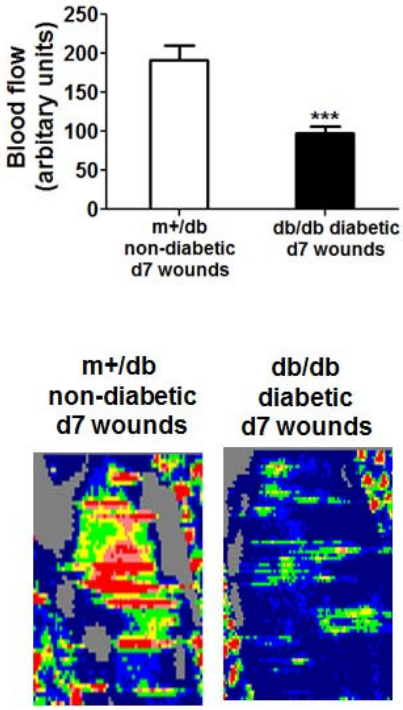

(B)

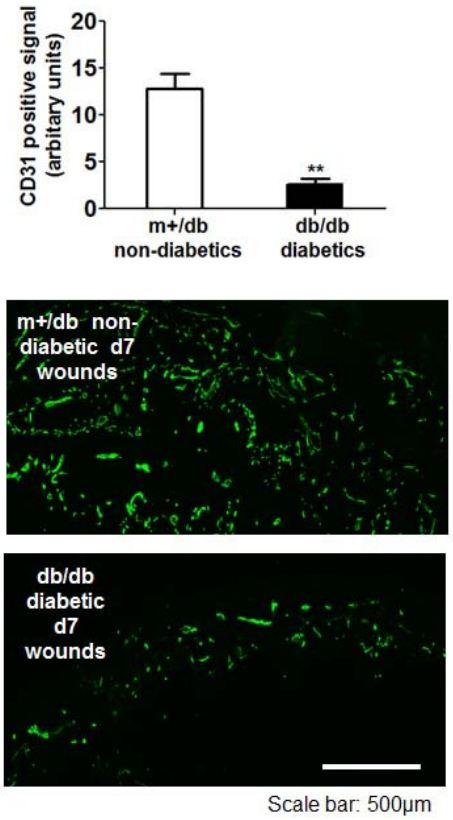

Supplemental Figure XIII

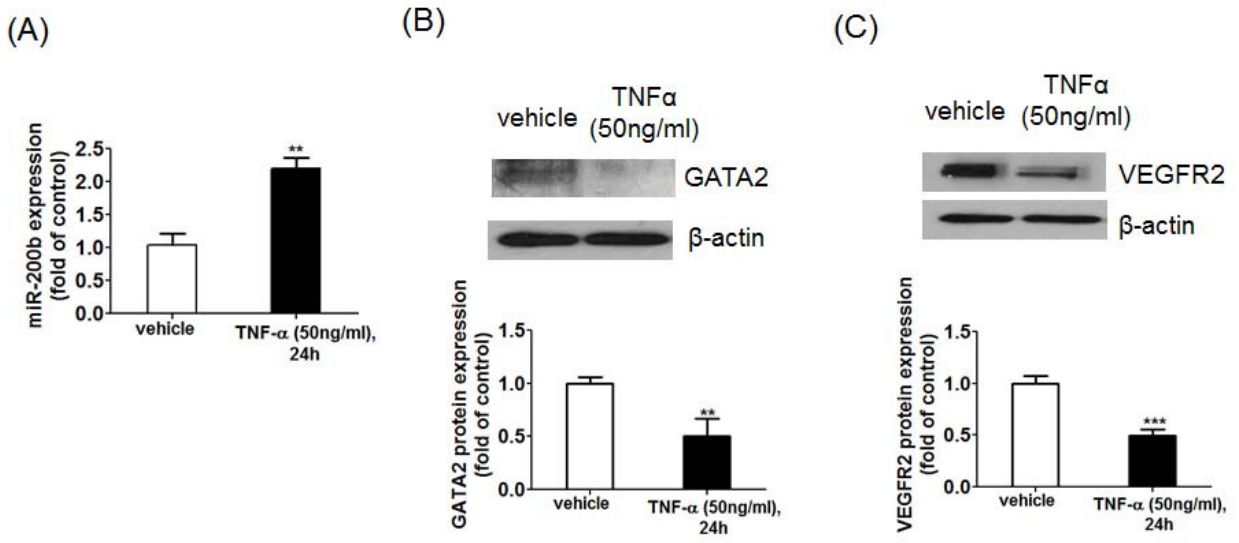

Supplemental Figure XIV

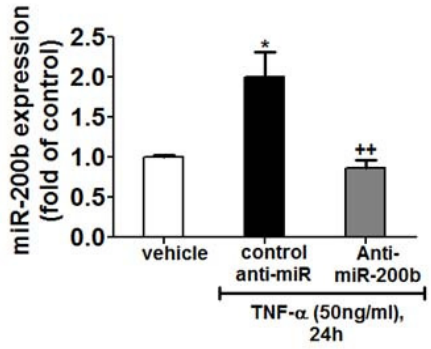

Supplemental Figure XV

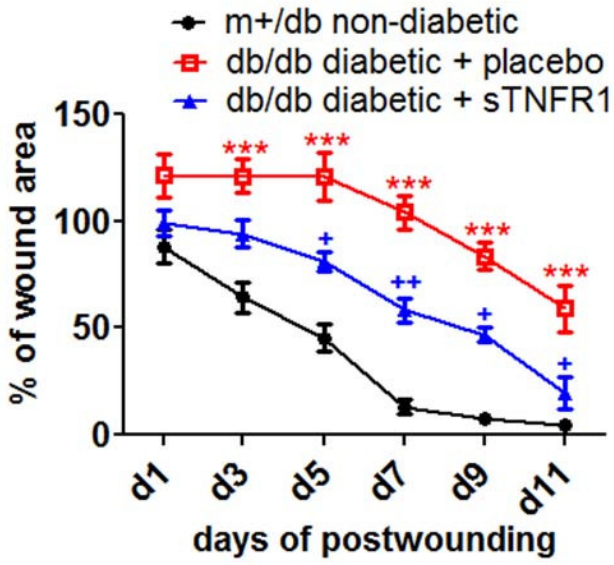

Supplemental Figure XVI

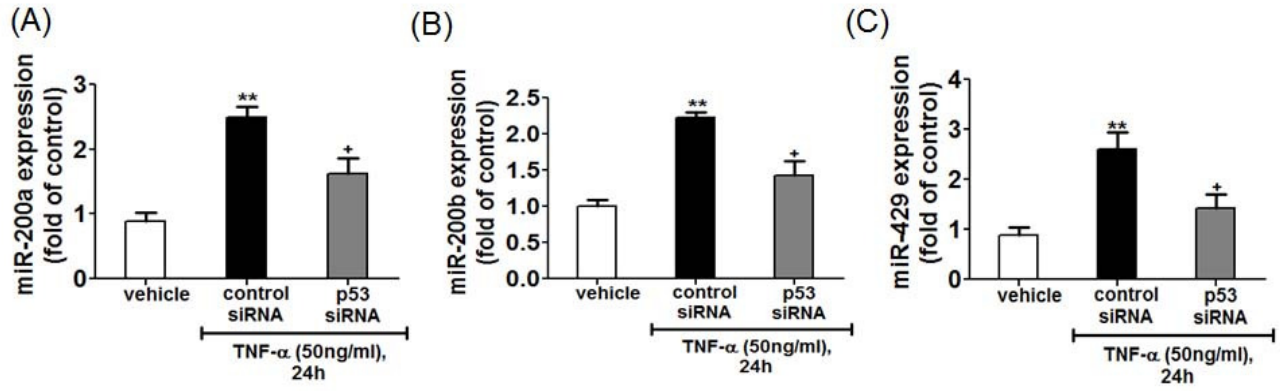

Supplemental Figure XVII